# Organic Light-Emitting Materials Based on Bis(arylacetylide)platinum(II) Complexes Bearing Substituted Bipyridine and Phenanthroline Ligands: Photo- and Electroluminescence from $^3$MLCT Excited States

**Siu-Chung Chan,[a] Michael C. W. Chan,[a] Yue Wang,[b] Chi-Ming Che,*[a] Kung-Kai Cheung,[a] and Nianyong Zhu[a]**

**Abstract:** We present the synthesis and photophysical and electroluminescent properties for a series of platinum(II) $\alpha$-diimine bis(arylacetylide) complexes. The molecular structures of five derivatives have been elucidated by X-ray crystallography. Intermolecular $\pi-\pi$ interactions (between aromatic diimine and phenylacetylide moieties) are apparent in the crystal lattices of two of these. All bis(phenylacetylide) derivatives exhibit intense triplet metal-to-ligand charge transfer (MLCT) photoluminescence in the solid state and in fluid solutions at room temperature. The impact of different solvents, substituents on the diimine ligands, and complex concentrations upon their emissive behavior have been examined and demonstrates that their emission energies can be systematically modified. Application of the $^3$MLCT excited state of the [Pt($\alpha$-diimine)(C≡CPh)$_2$] materials in single- and double-layer organic light-emitting devices are described. The bis(butadiynyl) complex [Pt(4,4′-dtbpy)(C≡C−C≡CPh)$_2$] (dtbpy = 4,4′-di-*tert*-butyl-2,2′-bipyridine) displays strong solid-state and solution phosphorescence at 77 and 298 K; the associated excited state is proposed to arise from both acetylenic $^3\pi\pi^*$(C≡C−C≡CPh) and $^3$MLCT [Pt → π*(diimine)] transitions.

**Keywords:** alkyne ligands · charge transfer · luminescence · phosphorescence · platinum

## Introduction

Hagihara and co-workers reported the first soluble metal poly-yne oligomers bearing [Pd(P*n*Bu$_3$)$_2$] and [Pt(P*n*Bu$_3$)$_2$] moieties in the main chain in 1975.[1] Since then, there has been considerable interest in transition metal acetylide complexes and polymers due to their potential applications in many fields of materials chemistry, including nonlinear optics, liquid crystals, conducting polymers, luminescent materials, and supramolecular chemistry.[2] The papers by Hagihara et al. continue to inspire interest in the electronic and spectroscopic properties of oligomeric and polymeric platinum acetylide species.[2e, 3] However, studies on the optoelectronic characteristics of these materials are sparse. The employment of metal–acetylide emitters in organic light-emitting devices (OLEDs) was demonstrated in our recent disclosure on the luminescent tetranuclear complex [Cu$_4$(C≡CPh)$_4$L$_2$] (L = 1,8-bis(diphenyphosphanyl)-3,6-dioxaoctane) as a dopant in poly(*N*-vinylcarbazole) (PVK).[4] The application of cyclometalated iridium(III) and platinum(II) compounds as electrophosphorescent dopants for OLEDs was published recently by Forrest and Thompson.[5]

The photoluminescence of discrete platinum acetylide complexes has been extensively investigated, but these are invariably supported by phosphane auxiliaries.[2c, 6] We reported the first luminescent platinum(II) acetylide complex with aromatic diimine ligands in 1994.[7] The [Pt(phen)(C≡CPh)$_2$] complex exhibits intense emission in fluid solution at room temperature which was attributed to a $^3$MLCT [Pt → π*(phen)] excited state. The incorporation of strong-field ligands (in this case acetylide), which are known to destabilize nonradiative ligand-field transitions in this class

[a] Prof. Dr. C.-M. Che, S.-C. Chan, Dr. M. C. W. Chan, Dr. K.-K. Cheung, Dr. N. Zhu
Department of Chemistry, The University of Hong Kong
Pokfulam Road, Hong Kong SAR (China)
Fax: (+852) 2857-1586
E-mail: cmche@hku.hk

[b] Prof. Y. Wang
Key Laboratory for Supramolecular Structure and Spectroscopy of Ministry of Education, Jilin University, Changchun 130023 (China)

Supporting information (UV absorption spectra for complexes **3a**–**f** in $CH_2Cl_2$; normalized absorption and emission spectra of **2a** in various solvents at 298 K; absorption, emission and excitation spectra of **2a** in $CH_2Cl_2$; solid-state emission spectra of $\mathbf{3f_p}$ and $\mathbf{3f_c}$ at 298 and 77 K; transient difference absorption spectra of **2a** and **4**; cyclic voltammogram of **2a** in DMF; cyclic voltammogram of wave 1 of **2a** in DMF at various scan rates; EL and PL spectra of **3b** and **3f**; current-voltage and luminance-voltage plots for devices based on **2a**, **3b** and **3f**; transient difference absorption data for **2a**, **2b**, **2d**, **3c**, **3d** and **4**; electrochemical data for **2**–**4**; luminous efficiency data for single and double-layer devices based on **2a**, **2b**, **2d**, **3b** and **3f**.) for this article is available on the WWW under http://www.wiley-vch.de/home/chemistry/ or from the author.



0947-6539/01/0719-4180 $ 17.50+.50/0

of luminophores,[8] is an important fundamental design consideration. Subsequent synthetic and spectroscopic investigations on platinum(II) diimine bis(acetylide) and related derivatives have appeared in the literature.[9, 10] Eisenberg and co-workers recently probed the excited-state properties of [Pt(diimine)(C≡CAr)$_2$] complexes by systematic ligand modification.[11] The emitting state was assigned as Pt → π*(diimine) $^3$MLCT in agreement with our original proposal,[7] and a correlation between the emission energy and the electron-withdrawing nature of the diimine auxiliary was observed. However, there has been no report on the development of these complexes towards applications as photonic materials.

Herein, we discuss a series of platinum(II) bis(phenylacetylide) complexes with different alkyl- and aryl-substituted 2,2′-bipyridyl (bpy) and 1,10-phenanthroline (phen) ancillary ligands (Scheme 1). By varying the N donor, we have been able to fine-tune their $^3$MLCT excited-state properties. These complexes are strong emitters in the solid state and in fluid solutions, and their electroluminescent (EL) properties have been studied in order to evaluate their suitability as OLED materials. Significantly, the bis(butadiynyl) derivative [Pt(4,4′-dtbpy)(C≡C−C≡CPh)$_2$] has also been synthesized. Our observations indicate that the parentage of the lowest energy emissive excited state for this species involves both $^3$[π → π*(C≡C−C≡CPh)] and $^3$[Pt → π*(diimine)] and depends on the emission environment (i.e. temperature and medium).

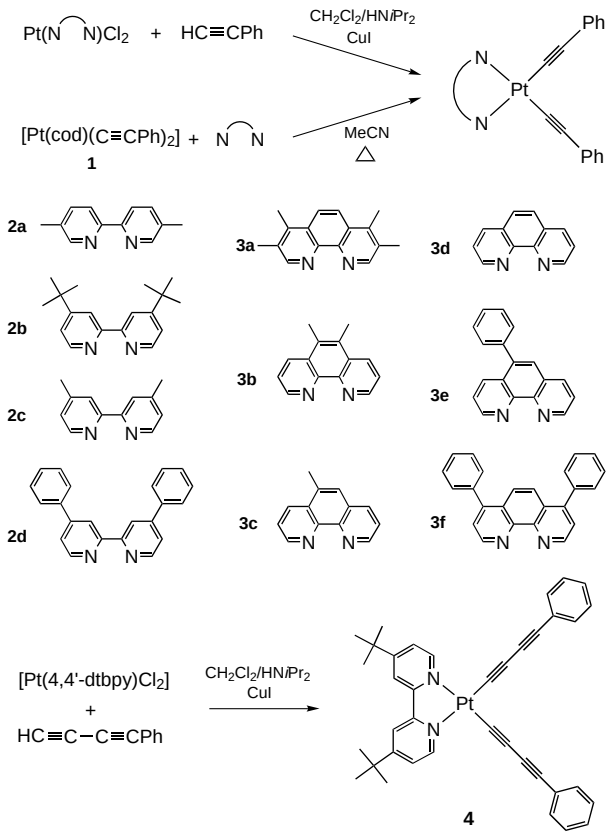


Scheme 1. Synthetic methodology.

## Results and Discussion

**Synthesis and characterization**: According to Sonogashira et al.,[12] platinum(II) arylacetylide complexes can be prepared by the reaction of $PtL_2Cl_2$ (L = phosphane donor) with organic arylacetylenes in $CH_2Cl_2$/HN*i*Pr$_2$ in the presence of a catalytic amount of copper iodide. Another synthetic route, which was reported by Cross et al.,[13] involves the displacement of the labile 1,5-cyclooctadiene (cod) group from the precursor [Pt(cod)(C≡CPh)$_2$] (**1**) using selected donor ligand(s). Herein, both methods were adopted to synthesize a range of bis(arylacetylide) Pt$^{II}$ complexes bearing different diimine auxiliaries (Scheme 1). The Sonogashira procedure generally affords better yields for substituted bpy derivatives (**2a**–**c**). The Cross method was employed for phen complexes (**3a**–**f**, plus **2d**), although the tendency of the [Pt(cod)(C≡CPh)$_2$] precursor to decompose at elevated temperatures resulted in low product yields for methyl- and phenyl-substituted species. The bis(phenylbutadiynyl) complex [Pt(4,4′-dtbpy)(C≡C−C≡CPh)$_2$] (**4**) was prepared in 86% yield by treatment of [Pt(4,4′-dtbpy)Cl$_2$] with PhC≡C−C≡CH in the presence of $CH_2Cl_2$/HN*i*Pr$_2$/CuI. All complexes are stable in the solid state and in dichloromethane solutions for several days at room temperature in the absence of light. The IR spectra for both the **2** and **3** series of complexes display two sharp bands at about 2120 and 2100 cm$^{-1}$, which correspond to the symmetric ($\nu_s$) and asymmetric ($\nu_{as}$) C≡C stretches of *cis*-phenylacetylide ligands. Complex **4** exhibits two IR bands at 2181 and 2067 cm$^{-1}$ and two Raman peaks at 2187 and 2070 cm$^{-1}$, which are assigned to the C≡C stretches. The $^{13}$C NMR chemical shifts of the acetylenic carbon atoms are comparable in the **2** and **3** series and are observed at around $\delta = 102$ and 87 for $C_\alpha$ and $C_\beta$, respectively. For complex **4**, relatively upfield chemical shifts at $\delta = 87.7$ ($C_\alpha$), 83.2 ($C_\beta$), 78.7 ($C_\gamma$), and 70.4 ($C_\delta$) are observed for the butadiynyl carbon atoms.

**Crystal structures**: The molecular structures of complexes **2b**·$CH_2Cl_2$, **2c**, **2d**·$CH_2Cl_2$ (Figure 1), **3e**·$CH_3CN$ (Figure 2) and **3f**·$(CH_2Cl_2)_{0.75}$ have been elucidated by X-ray crystallography. Crystal data and selected bond lengths and angles for **2d** and **3e** are listed in Table 1 and Table 2, respectively.

**Abstract in Chinese:**

本文報導了一系列 α－二亞胺雙（芳香乙炔）合鉑（II）絡合物的合成，光物理及電致發光性質。五個衍生物的分子結構由 X－射線晶體衍射的方法確定，其中兩個化合物的晶格中有明顯的分子間（芳香二亞胺與苯乙炔間）π－π 相互作用。所有雙（苯乙炔）衍生物在室溫狀態下固体及溶液中均具有較強的金屬－配体電荷轉移三線態 ($^3$MLCT) 光致發光性質。我們還研究了不同溶劑、取代基及絡合物濃度對其發光性質的影響，結果表明絡合物的發射能量可以通過以上方式進行系統地調節。另外本文還報導了α－二亞胺雙（苯乙炔）合鉑（II）材料 $^3$MLCT 激發態在單層和雙層有機發光器件上的應用。我們還發現 Pt(4,4′–dtbpy)(C≡C–C≡CPh)$_2$ 絡合物在室溫和 77 K 狀態下的固體及溶液中都表現出較強的磷光發射；該發射來自于炔化物 (C≡C–C≡CPh) 的 $^3$ππ* 和 $^3$MLCT [Pt→π*(二亞胺)] 的激發態。

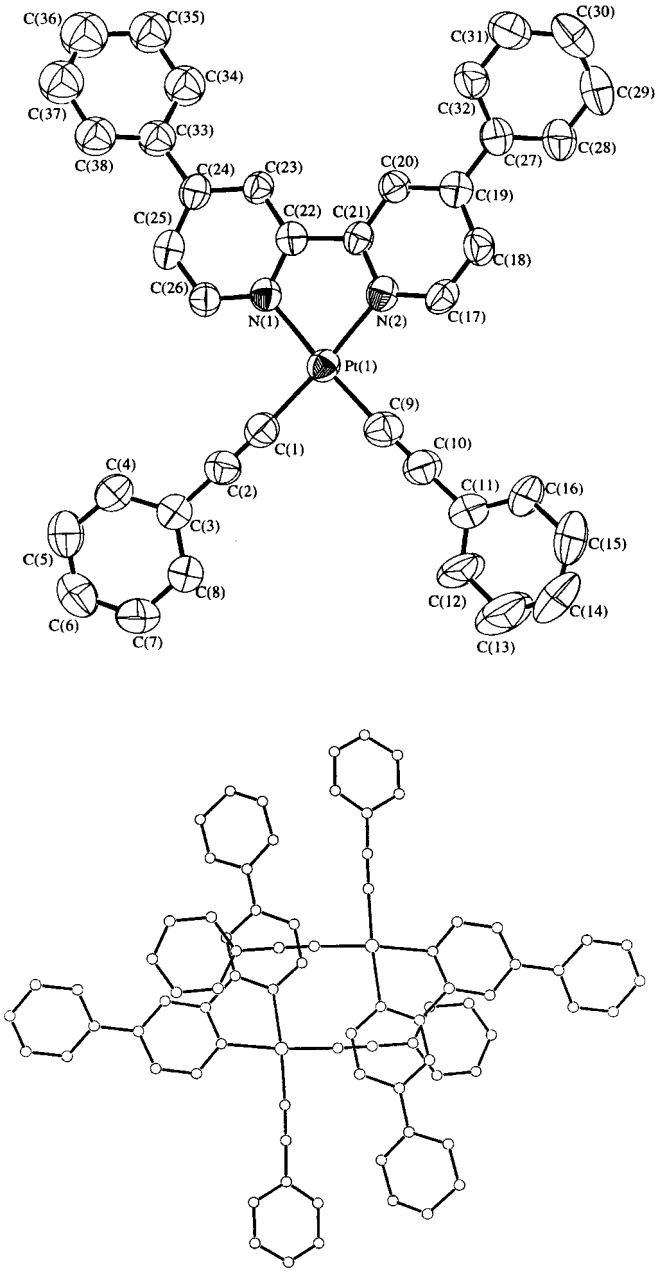




Figure 1. Top: Perspective view of **2d** (50% probability ellipsoids). Bottom: Stacking diagram showing $\pi-\pi$ interactions between phenylacetylide moieties and bipyridine fragments.

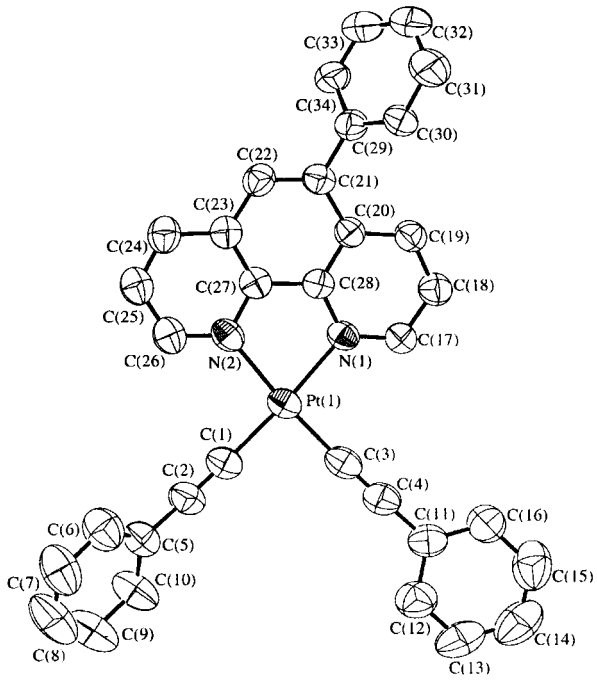


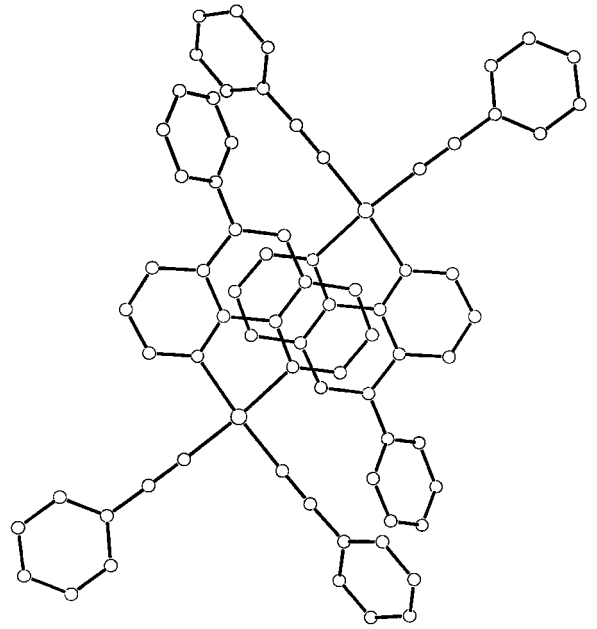

Figure 2. Top: Perspective view of **3e** (50% probability ellipsoids). Bottom: Stacking diagram showing $\pi-\pi$ interactions between (1) phen ligands, and (2) 5-Ph and C≡C–*Ph* moieties.

The Pt–N bond lengths observed in this report vary between 2.050(6) and 2.076(5) Å and are marginally longer than those of [Pt($\alpha$-diimine)$Cl_2$] ($\alpha$-diimine = 5,5′-dimethyl-2,2′-bipyridine (5,5′-dmbpy) (2.015 Å) and 3,3′-$(CH_3CO_2)_2$bpy (1.992 Å)).[8] These slight elongations reflect the greater trans influence of phenylacetylide in comparision to chloride. The Pt–C bond lengths (mean: 1.957 (**2b**), 1.963 (**2c**), 1.954 (**2d**), 1.944 (**3e**), and 1.964 Å (**3f**)) are within the range reported for platinum(II) diimine bis(acetylide) complexes,[7, 9a, 10c, 11a] and approach the Pt–C(phenyl) bond lengths in [Pt(dpp)$Ph_2$] (1.967(8) and 2.013(7) Å, dpp = 2,3-bis(2-pyridyl)pyrazine).[9a] The bond lengths between the acetylenic carbon atoms (1.169(9) – 1.219(8) Å) are surprisingly similar to those (1.203(14) – 1.24(2) Å) involved in $\eta^2$ coordination to metal thiocyanates in [Pt(4,4′-dtbpy)(C≡CR)$_2$M(SCN)] (R = $C_6H_4Me$, $SiMe_3$; M = Cu, Ag respectively).[10b] For **2d**, **3e** and **3f**, the phenyl substituents are rotated out of plane of the attached diimine ligand, and the corresponding (mean) dihedral angles are 31.7, 50.2 and 54.0°, respectively.

Significantly, multiple close intermolecular contacts are revealed upon inspection of the crystal lattice in **2d** (e.g. C(1)···C(25′) 3.580(9), C(1)···C(26′) 3.293(9), C(1)···N(1′) 3.595(8) Å). These distances are sufficiently short for $\pi-\pi$ interactions,[14] and indeed $\pi$ stacking of the acetylide and phenyl moieties with the bipyridine group is apparent



0947-6539/01/0719-4182 $ 17.50+.50/0 *Chem. Eur. J.* **2001**, *7*, No. 19

Table 1. X-ray crystallographic data for **2d**·$CH_2Cl_2$, and **3e**·$CH_3CN$.

| Compound | **2d**·$CH_2Cl_2$ | **3e**·$CH_3CN$ |
|---|---|---|
| chemical formula | $[C_{39}H_{28}N_2Cl_2Pt]$ | $[C_{36}H_{25}N_3Pt]$ |
| formula weight | 790.66 | 694.70 |
| crystal size [mm] | 0.4 × 0.1 × 0.1 | 0.25 × 0.15 × 0.07 |
| crystal system | monoclinic | monoclinic |
| space group | $P2_1/n$ (no. 14) | $P2_1/c$ (no. 14) |
| $a$ [Å] | 9.823(3) | 9.373(2) |
| $b$ [Å] | 24.038(4) | 16.625(3) |
| $c$ [Å] | 14.148(2) | 18.612(3) |
| $\alpha$[°] | 90.0 | 90.0 |
| $\beta$[°] | 103.46(2) | 91.87(2) |
| $\gamma$[°] | 90.0 | 90.0 |
| $V$ [Å$^3$] | 3249.1(10) | 2898.7(8) |
| $Z$ | 4 | 4 |
| $\rho_{calcd}$ [g cm$^{-3}$] | 1.616 | 1.592 |
| $\mu$ [cm$^{-1}$] | 44.96 | 48.50 |
| $2\theta_{max}$ | 50 | 51 |
| temperature [K] | 301 | 301 |
| $F$(000) | 1552 | 1360 |
| no. of unique data ($R_{int}$) | 5875 (0.037) | 5561 (0.046) |
| no. of obsd. data [$I \geq 3\sigma(I)$] | 3554 | 4030 |
| no. of variables | 383 | 346 |
| $R$[a] | 0.028 | 0.032 |
| $Rw$[b] | 0.034 | 0.044 |
| GoF[c] | 1.29 | 1.54 |

[a] $R = \Sigma||F_o| - |F_c||/\Sigma|F_o|$. [b] $Rw = [\Sigma w(|F_o| - |F_c|)^2/\Sigma w|F_o|^2]^{1/2}$. [c] $GoF = [\Sigma w(|F_o| - |F_c|)^2/(n-p)]^{1/2}$.

Table 2. Selected bond lengths [Å] and angles [°] of **2d**·$CH_2Cl_2$ and **3e**·$CH_3CN$.

| **2d**·$CH_2Cl_2$ | | **3e**·$CH_3CN$ | |
|---|---|---|---|
| Pt(1)–N(1) | 2.059(5) | Pt(1)–N(1) | 2.074(4) |
| Pt(1)–N(2) | 2.059(5) | Pt(1)–N(2) | 2.066(4) |
| Pt(1)–C(1) | 1.961(7) | Pt(1)–C(1) | 1.951(6) |
| Pt(1)–C(9) | 1.946(7) | Pt(1)–C(3) | 1.937(7) |
| C(1)–C(2) | 1.188(8) | C(1)–C(2) | 1.209(7) |
| C(9)–C(10) | 1.215(9) | C(3)–C(4) | 1.219(8) |
| C(2)–C(3) | 1.434(9) | C(2)–C(5) | 1.428(8) |
| C(10)–C(11) | 1.425(9) | C(4)–C(11) | 1.423(9) |
| N(2)-Pt(1)-C(1) | 174.2(2) | N(1)-Pt(1)-C(1) | 174.4(2) |
| Pt(1)-C(1)-C(2) | 177.5(6) | Pt(1)-C(1)-C(2) | 176.2(5) |
| C(1)-C(2)-C(3) | 178.4(7) | C(1)-C(2)-C(5) | 176.3(7) |
| N(1)-Pt(1)-C(9) | 175.4(2) | N(2)-Pt(1)-C(3) | 174.7(2) |
| Pt(1)-C(9)-C(10) | 177.5(6) | Pt(1)-C(3)-C(4) | 178.0(5) |
| C(9)-C(10)-C(11) | 178.9(8) | C(3)-C(4)-C(11) | 177.3(7) |
| C(1)-Pt(1)-C(9) | 88.8(3) | C(1)-Pt(1)-C(3) | 90.0(2) |
| N(1)-Pt(1)-C(1) | 95.8(2) | N(2)-Pt(1)-C(1) | 95.2(2) |

(Figure 1, bottom). Similarly, π–π interactions are also observed between adjacent phen ligands and between the 5-Ph and C≡C–*Ph* rings in **3e** (bottom of Figure 2, e.g. N(2)···C(23′) 3.478(7), C(10)···C(33′) 3.53(1), C(24)···C(27′) 3.574(8), C(25)···C(28′) 3.478(8) Å). No π stacking is evident in the crystal structures of **2b**, **2c** and **3f**. We have recently noted for several luminescent $Pt^{II}$ complexes that π–π contacts detected in the solid-state structure have direct impact upon emissive properties.[15] The consequences of the intermolecular interactions observed in this work upon luminescent characteristics will be described later.

**UV absorption spectroscopy**: The UV/Vis absorption data are summarized in Table 3, and the corresponding spectra for complexes **2a**–**d** and **4** in dichloromethane are shown in Figure 3 (see Supporting Information for the **3** series). All

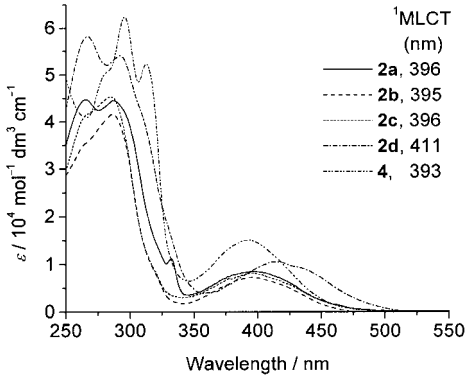


Figure 3. UV/Vis absorption spectra for complexes **2a**–**d** and **4** in dichloromethane at 298 K (wavelengths of the lowest energy absorption bands are listed).

complexes show intense absorption bands at 250–350 nm ($\varepsilon > 10^4$ mol$^{-1}$ dm$^3$ cm$^{-1}$) that are assigned to the intraligand transition ($^1$IL) of the diimine and/or arylacetylide ligands. The singlet π → π* transition of the phenylacetylide group has been observed at $\lambda < 300$ nm (i.e. for $[Cy_3PAuC{\equiv}CPh]$, $\lambda_{max}$ = 256, 267, 281, 290(sh)).[16] The high-energy absorptions in this study do not exhibit significant solvatochromic effects. The [Pt → π*(C≡CPh)] MLCT band (as assigned for $[Pt(PEt_3)_2(C{\equiv}CPh)_2]$ at $\lambda_{max} = 328$ nm)[17] presumably occurs in the UV region and is masked by the $^1$IL absorption.

Table 3. Photophysical data in solution.

| Complex | $\lambda_{abs}$ [nm] ($\varepsilon$ [mol$^{-1}$dm$^3$cm$^{-1}$]) | $\lambda_{em}$ [nm] ($\tau_o$ [$\mu$s][a], $\Phi_{em}$[b]) $CH_2Cl_2$ at 298 K | $\lambda_{em}$ [nm] ($\tau$ [$\mu$s])[a] EtOH/MeOH (4:1 v/v) at 77 K | $k_q \times 10^9$ s$^{-1}$ |
|---|---|---|---|---|
| **2a** | 265 (44700), 286 (44500) 332 (11300), 396 (8500) | 545 (1.6, 0.64) | 495 (max, 4.7), 527 | 2.79 |
| **2b** | 287 (41600), 396 (7300) | 554 (1.3, 0.50) | 489 (max, 3.8) | 0.29 |
| **2c** | 284 (45400), 395 (8200) | 554 (1.2, 0.50) | 499 (max, 4.5), 530 | 2.20 |
| **2d** | 266 (58200), 292 (54100) 411 (10600) | 580 (1.0, 0.35) | 528 (max, 5.7), 564 | 1.84 |
| **3a** | 280 (62400), 365 (10600) | 522 (2.7, 0.60) | 488 (max, 11.6), 522, 558 | 2.90 |
| **3b** | 279 (55700), 377 (7000), 404 (7900) | 554 (2.3, 0.60) | 528 (max, 6.7) | 3.46 |
| **3c** | 276 (57800), 400 (7600) | 558 (2.0, 0.49) | 532 (max, 1.4) | 3.86 |
| **3d** | 268 (58400), 396 (7900) | 561 (1.9, 0.42) | 506 (max, 6.8), 539 | 3.68 |
| **3e** | 279 (59700), 401 (8800) | 563 (2.0, 0.53) | 514 (max, 9.6), 548, 588 | 2.32 |
| **3f** | 283 (64700), 385 (11300) | 570 (2.8, 0.49) | 532 (max, 13.8), 569 | 1.36 |
| **4** | 296 (61300), 312 (51400), 393 (14900) | 536 (1.1, 0.57) | 482 (max, 13.2), 519, 538 | 1.00 |

[a] $\tau_o$ is the lifetime at infinite dilution. [b] $\Phi_o$ is the emission quantum yield at y-axis value in extrapolation of Stern-Volmer plot.

A broad absorption with $\lambda_{max}$ ranging from 365–411 nm was previously assigned in our earlier paper[7] as a singlet MLCT [5d(Pt) → π*(diimine)] transition. We note that the $^1$MLCT [Pt → π*(5-mphen)] transition for [Pt(5-mphen)-(C≡N)$_2$] appears at 347 nm ($\varepsilon_{max} = 1.48 \times 10^3$ mol$^{-1}$dm$^3$cm$^{-1}$ in acetonitrile[18]; 5-mphen = 5-methyl-1,10-phenanthroline), and is significantly blue-shifted from the analogous transition in [Pt(5-mphen)(C≡CPh)$_2$] ($\lambda_{max} = 400$ nm in dichloromethane). This can be attributed to stronger σ donation by phenylacetylide with respect to cyanide, causes greater destabilization of the Pt(5d) HOMO and results in lowering of the MLCT transition energy.

The solvatochromic shift of the lowest-energy absorption and emission bands of **2a** (see Supporting Information), **2b**, **2c** and **4** in various solvents (Table 4) is indicative of their MLCT nature. The $^1$MLCT absorption maximum of **2a** in methanol (384 nm) is red-shifted (2118 cm$^{-1}$) to 418 nm in benzene. Comparable results have been reported for other Pt$^{II}$ α-diimine bis(arylacetylide) systems.[7, 11a] The solvatochromic shifts for the 4,4′-dtbpy congeners **2b** and **4** are comparable in nonprotic solvents, although the absorption maxima of complex **4** in MeOH (377 nm) and in EtOH (383 nm) unusually exhibit red shifts with respect to the maxima in acetonitrile (374 nm). The minor blue-shift of the singlet MLCT band of **4** relative to **2b** can be rationalized by the presence of the more conjugated C≡C–C≡CPh ligands. This is expected to stabilize the $d_\pi$(Pt) orbital, which results in a lowering of the HOMO level and thus an increase of the MLCT energy. Similar observations have been reported by Yam and co-workers on related rhenium(I) triynyl complexes.[19]

Table 4. Photophysical data for MLCT band of **2a**, **2b**, **2c**, and **4** in various solvents at 298 K.

| Solvent | **2a** | | **2b** | | **2c** | | **4** | |
|---|---|---|---|---|---|---|---|---|
| | $\lambda_{abs}$ [nm] | $\lambda_{em}$ [nm] | $\lambda_{abs}$ [nm] | $\lambda_{em}$ [nm] | $\lambda_{abs}$ [nm] | $\lambda_{em}$ [nm] | $\lambda_{abs}$ [nm] | $\lambda_{em}$ [nm] |
| benzene | 418 | 553 | 419 | 561 | 422 | 564 | 417 | 541 |
| $CH_2Cl_2$ | 396 | 545 | 396 | 554 | 395 | 554 | 392 | 536 |
| acetone | 397 | 549 | 394 | 558 | 397 | 558 | 386 | 535 |
| DMF | 394 | 543 | 391 | 554 | 392 | 554 | 382 | 530 |
| $CH_3CN$ | 386 | 544 | 385 | 552 | 386 | 554 | 374 | 528 |
| MeOH | 384 | 547 | 382 | 557 | 383 | 554 | 377[a] | 537[b] |

[a] 383 nm in EtOH. [b] 548 nm in EtOH.

**Emission spectroscopy:** All α-diimine complexes are emissive both in fluid solution and solid state at ambient temperature and 77 K (Table 3 and Table 5). With the exception of complex **4**, which will be described separately, all complexes show similar emissive properties, and **2a** is selected as a representative example to be discussed in detail. At 298 K, a solution of complex **2a** in dichloromethane displays a broad and structureless emission band at $\lambda_{max} = 545$ nm. The excitation spectra of **2a** (see Supporting Information) is similar in appearance to the absorption spectra at low concentration, which indicates efficient intersystem crossing from the high-energy electronic excited state to the emitting state. Therefore, the origin of this emission band is assigned as a triple MLCT $^3$[5d(Pt) → π*(diimine)] excited state. Unlike the $^1$MLCT absorption band which displays discernible solvatochromic behavior, the solution emission maximum of **2a** shows minimal variation in different solvents (Table 4 and Supporting Information).

In accordance with the results of Eisenberg et al.,[11a] the solution emission maxima for both the **2** and **3** series of derivatives shift to lower energies as the electron-withdrawing nature of the substituted bipyridine and phenanthroline ligands, respectively, increase (Table 3). Assuming all complexes exhibit pure $^3$MLCT emission and the complexation of diimine ligands does not affect the Pt-based HOMO level, this result demonstrates that the electronic effect of the α-diimine ligands yields LUMO energy levels in the following descending order: 3,4,7,8,-tetramethyl-1,10-phenanthroline (tmphen) > 5,5′-dmbpy > 5,6-dimethyl-1,10-phenanthroline (5,6-dmphen) ≈ 4,4′-di-*tert*-butyl-2,2-′bipyridine (4,4′-dtbpy) ≈ 4,4′-dmbpy > 5-mphen > 4,7-diphenyl-1,10-phenanthroline (dpphen) > 4,4′-diphenyl-2,2′-bipyridine (dpbpy). The ability to fine-tune excited-state energies is important for applications as light-emitting materials. For complexes supported by different α-diimine ligands (Figure 4), the emission energies can be systematically modified over a wide range (≈1920 cm$^{-1}$).

The self-quenching of photoluminescence of Pt$^{II}$ diimine complexes in solution has previously been reported and ascribed to excimer formation.[11b, 15a] The self-quenching rate constant ($k_q$) can be calculated from the Stern–Volmer equation and the results are listed in Table 3. Smaller $k_q$ values are observed for bulky diimine groups (e.g. lowest $k_q$ for 4,4′-dtbpy derivatives **2b** and **4**) as expected.

Table 5. Solid-state photophysical data.

| Complex | Nature | $\lambda_{em}$ [nm] ($\tau_o$ [μs])[a] Solid at 298 K | $\lambda_{em}$ [nm] ($\tau_o$ [μs]) Solid at 77 K | $\Phi_{ss}$[a] [%] |
|---|---|---|---|---|
| **2a** | yellow crystals | 510, 536 (max, 0.61) | 501, 535 (max, 2.8), 558 | 8.24 |
| **2b** | yellow crystals | 527 (max, 0.42), 565 | 502 (max, 2.3), 535, 572 | 6.35 |
| **2c** | yellow crystals | 526 (max, 0.45), 562 | 493, 522 (max, 2.2), 557 | 4.89 |
| **2d** | orange crystals | 589 (max, 0.66) | 552 (max, 2.4), 592 | 2.64 |
| **3a** | yellow crystals | 533 (max, 0.64), 568 | 516, 551 (max, 5.3) | 4.40 |
| **3b** | shiny orange powder | 563 (max, 0.38), 601 | 555 (max, 1.8), 595 | 1.84[b] |
| **3c** | yellow powder | 570 (max, 0.11) | 559 (max, 2.5), 601 | 2.22 |
| **3d** | yellow crystals | 521 (max, 0.20), 556 | 508 (max, 2.5), 542, 580 | 2.70 |
| **3e** | yellow crystals | 556 (max, 0.31), 648 | 527 (max, 2.1), 564, 605 | 1.85 |
| **3f$_p$** | orange powder | 546, 584 (max, 0.20) | 538 (max, 0.98 & 6.3[c]), 580 | 0.66 |
| **3f$_c$** | deep orange crystals | 554, 620 (max, 2.06) | 559, 580, 612 (max, 0.50 & 5.3[c]), 661 | 0.66 |
| **4** | yellow powder | 505, 539, 600 (max, 0.12) | 489 (max, 0.96), 532, 546, 603 | 0.13 |

[a] $\Phi_{ss}$ = solid-state emission quantum yield. [b] **3b**:KBr (1:20) mixture. [c] Second-order decay.



0947-6539/01/0719-4184 $ 17.50+.50/0 *Chem. Eur. J.* **2001**, *7*, No. 19

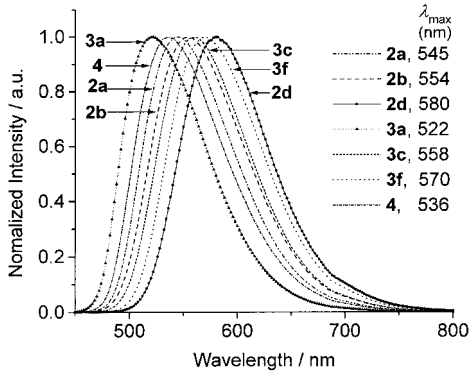


Figure 4. 298 K emission spectra for selected complexes in dichloromethane, illustrating the tunable range of emission energies.

For solid-state and ethanol–methanol (4:1 v/v) glassy emissions at 77 K, the **2** and **3** series of complexes exhibit vibronic structure with vibrational progressions of around 1250 $cm^{-1}$ (Figure 5 for **2a**), which is characteristic of the ring-breathing mode of polypyridyl ligands. These vibronic emissions provide further evidence in support of the involvement of the diimine ligand in the emissive excited state (i.e. $^3$[5d(Pt) → π*(diimine)]).

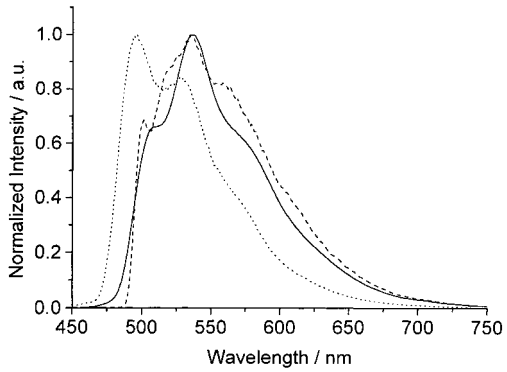


Figure 5. 298 (——) and 77 K (----) solid-state emission of **2a**; ethanol/methanol (4:1 v/v) emission at 77 K (••••).

With the exception of **2d**, **3c**, **3e**, and **3f**$_c$ (deep orange crystalline form of **3f**), both series of derivatives (**2** and **3**), including **3f**$_p$ (orange powder form of **3f**), display vibronically structured solid-state emissions at room temperature (Table 5). The phenyl-substituted phenanthroline complexes **3e** and **3f**$_c$ exhibit emission maxima at 648 and 620 nm respectively (see Supporting Information for 298 and 77 K solid-state emission spectra of **3f**$_p$ and **3f**$_c$), which are substantially red-shifted from their corresponding solution emissions (563 and 570 nm respectively). These low-energy emissions are ascribed to excimer formation arising from π–π stacking interactions in the solid state, as observed in the crystal lattice of **3e**·$CH_3CN$ (see above) and reported in our recent studies.[15] Based on the above hypothesis, it is therefore surprising that intermolecular π–π stacking is not observed in the crystal lattice of **3f**·$(CH_2Cl_2)_{0.75}$ and excimeric emissions are not detected even for high concentration ($10^{-3}$ M) solutions of **3f**. For this solid, we suggest that excimer formation only occurs in the unsolvated, amorphous form (i.e. **3f**$_c$) which exhibits a different packing arrangement from the solvated **3f**·$(CH_2Cl_2)_{0.75}$ lattice. A precedent for contrasting π-stacking conformations for solvated and unsolvated crystal structures was recently published for $Pt^{II}$ complexes derived from *trans*-cyclometalated 2,6-diphenylpyridine.[15e] Solid-state emission quantum yields were determined according to the method described by Wrighton and co-workers[20] and are listed in Table 5. The highest solid-state quantum yield of 8.2% was observed for **2a** and the lowest (0.13%) for **4**.

**Photoluminescence of [Pt(4,4′-dtbpy)(C≡C–C≡CPh)$_2$] (4):** The fluid emission of **4** (Figure 6) exhibits similar emission and excitation properties to that of the **2** and **3** series and is

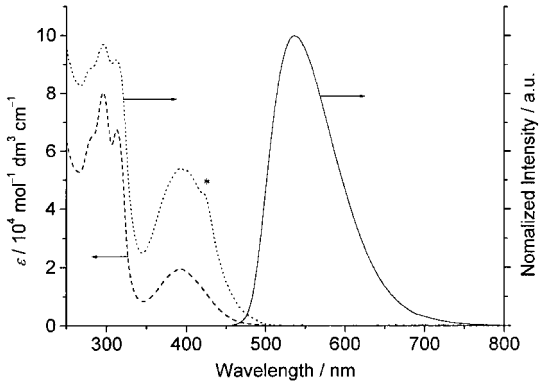


Figure 6. Absorption (----), emission (——) and excitation (••••) spectra of **4** in $CH_2Cl_2$ at 298 K (* indicates artifact).

assigned to a triplet [5d(Pt) → π*(diimine)] MLCT excited state. However, complex **4** (with *cis*-configured C≡C–C≡CPh moieties) displays different solid-state and glassy emissions (Figure 7) in comparison to the bis(phenylacetylide) ana-

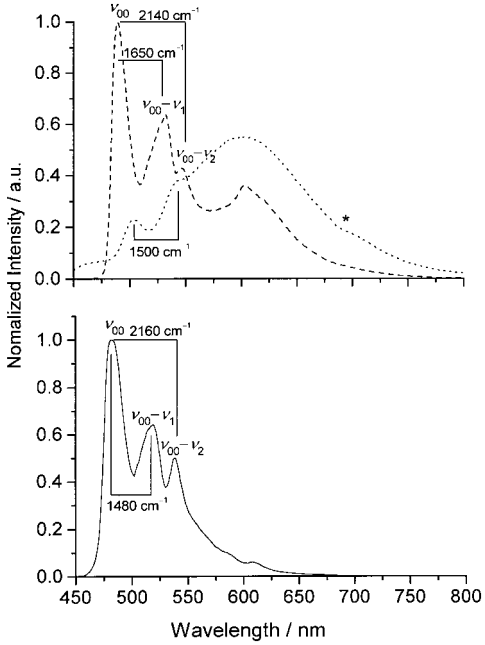


Figure 7. Top: solid-state emission of **4** at 298 (••••) and 77 K (----) (* indicates artifact). Bottom: ethanol/methanol (4:1 v/v) emission of **4** at 77 K (——).

logues. The 77 K solid-state emission spectrum of **4** is well-resolved. We reason that the low-energy shoulder at 603 nm is dominated by excimeric emission. The three peak maxima at 489 (max), 532 and 546 nm are tentatively assigned to a metal-perturbed triplet intraligand ($^3\pi\pi^*$) excited state that originates from the [C≡C−C≡CPh] moieties. The spacings are interpreted using two vibronic modes, namely $\nu_1$ and $\nu_2$, as shown in Figure 7 (top). The 1650 $cm^{-1}$ spacing correlates to the symmetric phenyl ring stretches, and the 2140 $cm^{-1}$ progression corresponds to ν(C≡C) and approaches the 2067 and 2181 $cm^{-1}$ bands observed in the IR spectrum. Significantly, the corresponding $^3\pi\pi^*$ emission for the phenylbutadiynyl group in [Au(C≡C−C≡CPh)($PCy_3$)] ($PCy_3$ = tricyclohexylphosphine) is slightly blue-shifted to $\lambda_{max}$ 463 (max), 486, 500, 516 nm[16] but otherwise is very similar to that of **4**. Likewise, these mixed spacings have also been observed in platinum(II)[6a] and silver(I)[21] arylacetylide complexes. The 298 K solid-state emission spectrum of **4** is poorly resolved; we assign the peak maxima at $\lambda_{max}$ 600 nm to excimeric emission, while the peaks at $\lambda_{max}$ 502 and 543 nm are tentatively attributed to the $^3(\pi^* \rightarrow \pi)$(C≡C−C≡CPh) transition.

The 77 K emission spectrum of **4** in an ethanol-methanol (4:1 v/v) glassy matrix (bottom of Figure 7) is similar to that of the solid state ($\nu_{00}-\nu_1 = 1480\ cm^{-1}$, $\nu_{00}-\nu_2 = 2160\ cm^{-1}$). A notable discrepancy is that the intensity of the emission band at $\lambda \sim 600$ nm is significantly lower in the glassy solution, and this is in agreement with the excimeric excited-state assignment.

We attribute the difference between the emissive excited states for complex **4** in 77 K solid state/alcoholic glass ($^3$[ππ*(C≡C−C≡CPh)]) and 298 K fluid ($^3$[5d(Pt) → π*(4,4′-dtbpy)]) to the influence of solvent molecules. We suggest that the energy levels of the two excited states are comparable. Solvent binding to the coordinatively unsaturated platinum center in the excited state will stabilize the [5d(Pt) → π*(4,4′-dtbpy)] MLCT state in solution. However, in solid or glassy media at low temperature, the MLCT state presumably occurs at a higher energy and the ππ* intraligand emission dominates.

**Triplet-state absorption spectroscopy:** The triplet-state absorption spectra for complexes **2a**, **2c**, **2d**, **3c**, **3d**, and **4** in degassed acetonitrile following pulse excitation at 355 nm have been studied with nanosecond transient absorption difference spectroscopy (see Supporting Information for details and spectra of **2a** and **4**). For the **2** and **3** series, the triplet-state absorption spectra are characterized by absorptions at ~340 nm and in the 430–470 nm region. The 340 nm band is assigned as originating from the α-diimine anion radical of the MLCT state.[22] Beyond 460 nm, the tailing effect of the intense phosphorescence causes a dramatic drop of the absorption and affects the assignment of the 430–470 nm band. Nevertheless, this absorption band is tentatively assigned to the triplet MLCT absorption since the transient absorption decay corresponds to the emission lifetime of the phosphorescence. The major difference for **4** is that the absorption band at 340 nm is noticeably smaller and the $^3$MLCT absorption band is blue-shifted to 415(sh) and 437 nm.

**Electrochemistry**: The cyclic voltammograms of all complexes are comparable (see Supporting Information). In DMF/0.1 M TBAP, all complexes show two couples at $E_{1/2} = -1.65$ to $-2.00$ (reversible, wave 1) and $-2.25$ to $-2.55$ V (quasi-reversible, wave 2) versus $FeCp_2^{0/+}$, plus an irreversible wave at $E_{pa} = 0.31$ to 0.51 V versus $FeCp_2^{0/+}$ (wave 3). The $i_p^a/i_p^c$ ratio of wave 1 is close to unity and the plot of $i_p^c$ versus the square root of the scan rate is linear (see Supporting Information for **2a**). This suggests that wave 1 is a reversible one-electron reduction couple and it is thus assigned to the ligand-centered reduction of the diimine ligand [Eq. (1)].[10c, 23] Wave 2 (quasi-reversible reduction) and wave 3 (irreversible oxidation) are assigned to the second diimine reduction [Eq. (2)] and $Pt^{III}/Pt^{II}$ oxidation [Eq. (3)] respectively.

$$[Pt^{II}(\alpha\text{-diimine})(C{\equiv}CR)_2] + e^- \rightarrow [Pt^{II}(\alpha\text{-diimine}^-)(C{\equiv}CR)_2] \quad (1)$$

$$[Pt^{II}(\alpha\text{-diimine}^-)(C{\equiv}CR)_2] + e^- \rightarrow [Pt^{II}(\alpha\text{-diimine}^{2-})(C{\equiv}CR)_2] \quad (2)$$

$$[Pt^{II}(\alpha\text{-diimine})(C{\equiv}CR)_2] - e^- \rightarrow [Pt^{III}(\alpha\text{-diimine})(C{\equiv}CR)_2] \quad (3)$$

The $E_{pa3} - E_{pc1}$ values (see Supporting Information) represent the lowest charge separation potential of the [Pt(α-diimine)(C≡CR)$_2$] complexes. A qualitative relationship between the separation potential for each of the bipyridine and phenanthroline series and the respective emission energy is observed. This correlation signifies that the electron-withdrawing characteristics of the diimine ligands affect both the emission maxima and electrochemical properties of these bis(arylacetylide) complexes to a comparable extent.

**Electroluminescent properties: materials for OLEDs:** Although studies on bis(acetylide)platinum complexes supported by α-diimine ligands have appeared since our first report in 1994,[7] we are not aware of any attempts to develop these materials towards optoelectronic applications. The highly tunable orange-red emission energies of these luminescent complexes, plus their high quantum yields, make them suitable candidates as OLED emitters. Thus complexes **2a**, **2b**, **2d**, **3b**, or **3f** (10 wt %) and poly(*N*-vinylcarbazole) (PVK, 90 wt %) were incorporated by spin-coating into OLED devices and the electroluminescent (EL) characteristics were examined (see Supporting Information). The EL spectra for the single-layer devices (configuration: [ITO/PVK:**Pt**/Al]) of the five complexes are similar to the corresponding thin-film PL spectra (see Figure 8 for **2a**) with minor blue shifts (~5 nm) in the emission maxima. The single-layer EL device for **2a** is superior and exhibits a maximum luminance of 620 $cd\,m^{-2}$ at a driving voltage of 30 V and peak luminous efficiency of 0.10 $lm\,W^{-1}$ at luminance of 25 $cd\,m^{-2}$.

To enhance the EL brightness and efficiency of the devices, a double-layer device was formed by introducing an electron-transporting layer (ETL) between the [PVK:**Pt**] layer and the Al cathode. In this work, 2-(4-biphenyl)-5-(4-*tert*-butylphenyl)-1,3,4-oxadiazole (PBD) was selected as the ETL material since its LUMO level is lower than that of PVK. The relative energy levels of the OLED materials are depicted in Figure 9. The lower energy barrier for electron injection between Al



0947-6539/01/0719-4186 $ 17.50+.50/0 *Chem. Eur. J.* **2001**, *7*, No. 19

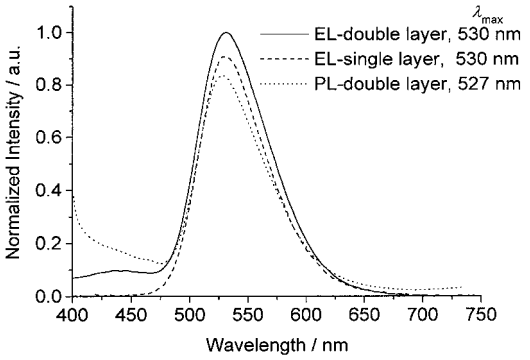


Figure 8. EL and PL spectra for devices based on **2a**.

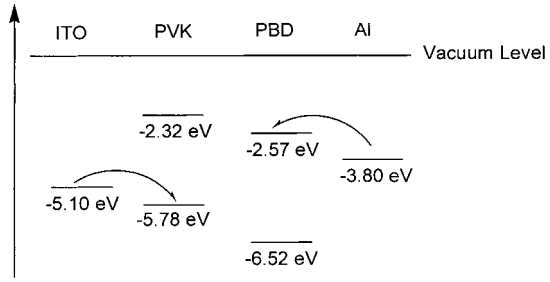


Figure 9. Energy diagrams of PVK, PBD and electrodes.

and PBD is expected to balance the rate of hole and electron injection into the emitter in order to achieve higher EL efficiency. In addition, PBD acts as a confinement layer to increase the distance between excitons and the cathode, at which nonradiative quenching can take place through physical and chemical interactions. The double-layer devices (configuration: [ITO/PVK:**Pt**/PBD/Al]) display significant improvements in EL performance in comparison to single-layer (see Supporting Information for details). In particular, the [ITO/PVK:**3f**/PBD/Al] device exhibits peak luminous efficiency of 1.33 $lm\,W^{-1}$ at 23 $cd\,m^{-2}$ and maximum luminance of 945 $cd\,m^{-2}$ at 28 V. The I-V-L characteristics of the double-layer device derived from **3f** are presented in Figure 10.

There is weak EL from the double-layer devices at ~420 nm which can be attributed to the PBD layer. EL from PVK is not observed in the single-layer devices, and this indicates efficient Förster energy transfer[24] from PVK to the Pt emitter. To confirm this, the PL spectra of single-layer films of [PVK:**Pt**] were recorded and indeed, only emission bands originating from the Pt complexes were detected. We note that significant overlap exists between the $^1$MLCT absorption bands of the $Pt^{II}$ complexes used in this EL study ($\lambda_{max} = 385–411$ nm) and the emission of PVK (400 nm), and this increases the likelihood for efficient singlet energy transfer.

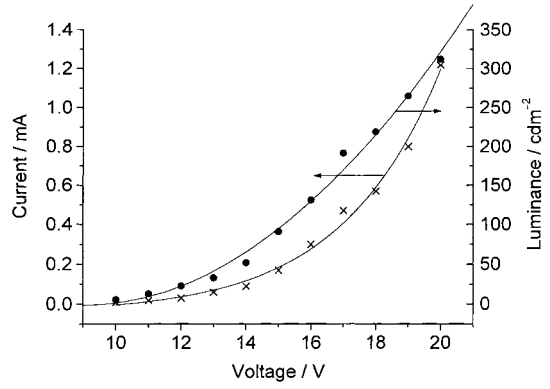


Figure 10. Current–voltage and luminance–voltage plots for the double-layer device of **3f**.

## Concluding Remarks

A series of highly photoluminescent and tunable bis(phenylacetylide)platinum(II) complexes supported by alkyl- and phenyl-substituted bpy and phen ligands have been synthesized. In accordance with Eisenberg's work,[11a] a correlation between the electron-withdrawing ability of the $\alpha$-diimine auxiliary and the emission energy, as well as the electrochemical data, is apparent, and this provides strong evidence to substantiate our original $^3$[5d(Pt) → π*(diimine)] excited-state assignment.[7] The preparation and photophysical behavior of the bis(phenylbutadiynyl) species **4** is significant because it appears that the nature of its lowest-energy excited state is not dominated by Pt → π*(diimine) MLCT. The blue-shift of its 298 K $^3$MLCT fluid emission relative to **2** is attributed to the delocalized nature of the butadiynyl moieties, which affords stabilization to the Pt-based HOMO. The 77 K solid-state and glassy photoluminescence of **4** is proposed to originate from a metal-perturbed $^3$[ππ*(C≡C–C≡CPh)] excited state.

Several new derivatives have been employed as electrophosphorescent emitters in single- and double-layer OLEDs. The good overlap observed between the absorption bands of the $Pt^{II}$ complexes and the PVK emission facilitates Förster energy transfer. There is no apparent trend between the photoluminescent quantum efficiency and electroluminescent luminous efficiency of these materials. While the performance of the devices described herein are limited, we have illustrated that these arylacetylide complexes warrant further investigations as OLED materials due to their tunable emission properties and their ability to mediate efficient energy transfer. The application of related electrophosphorescent emitters in high-efficiency OLEDs will be reported shortly.[25]

## Experimental Section

**Materials:** All chemicals and solvents (AR grade) for syntheses were used as received and the solvents for physical measurements were purified according to literature methods.[26] Dichloro(1,5-cyclooctadiene)platinum(II) [Pt(cod)$Cl_2$] (cod = 1,5-cyclooctadiene), phenylacetylene, potassium *tert*-butoxide, 4,4′-dimethyl-2,2′-bipyridine, 4,4′-diphenyl-2,2′-bipyridine, 1,10-phenanthroline monohydrate, 5,6-dimethyl-1,10-phenanthroline, 5-methyl-1,10-phenanthroline, 5-phenyl-1,10-phenanthroline, and 4,7-diphenyl-1,10-phenanthroline were purchased from Aldrich. 3,4,7,8-Tetramethyl-1,10-phenanthroline was purchased from Lancaster. [Pt(cod)(C≡CPh)$_2$] (**1**),[13] [Pt($\alpha$-diimine)$Cl_2$],[27] 5,5′-dimethyl-2,2′-bipyridine,[28] 4,4′-di-*tert*-butyl-2,2′-bipyridine[28] and 4-phenyl-1,3-butadiyne (HC≡C–C≡CPh)[29] were prepared by published methods. The synthesis of complexes **2b**,[10c, 11a] **2c**,[10a] **3c**,[11a] and **3d**[7, 11a] have been previously reported.

**Instrumentation**: $^1$H and $^{13}$C NMR spectra were recorded on Bruker DPX-300 or 500 multinuclear FT-NMR spectrometers with tetramethylsilane as the internal standard. Infrared spectra were obtained on a Bio-Rad FTs-

165 spectrometer in KBr. Raman spectra were recorded on a Perkin-Elmer Spectrum 2000 NIR FT-Raman. UV/Vis spectra were obtained on a Perkin-Elmer Lambda 19 UV/VIS/NIR spectrophotometer. Positive-ion FAB mass spectra were recorded on a Finnigan MAT95 mass spectrometer.

Steady-state emission and excitation spectra at 298 and 77 K were obtained on a Spex 1681 Flurolog-2 Model F111 spectrophotometer equipped with a Hamamatsu R928 PMT detector. The 77 K solid-state and [EtOH/MeOH (4:1 v/v)] emission and excitation spectra were recorded by loading the solid sample in a quartz tube inside a quartz-walled optical Dewar flask which was filled with liquid nitrogen. All solutions for photophysical measurements were degassed in a high-vacuum line with at least four freeze-pump-thaw cycles. Emission lifetimes were measured with a Quanta-Ray Q-switch DCR-3 Nd:YAG pulsed laser system.

Emission quantum yields were measured by the method of Demas and Crosby[30] using a degassed acetonitrile solution of $[Ru(bpy)_3]Cl_2$ (bpy = 2,2′-bipyridine) as the standard ($\Phi_r = 0.062$) and calculated by $\Phi_s = \Phi_r(B_r/B_s)(n_s/n_r)^2(D_s/D_r)$, where the subscripts s and r refer to the sample and reference standard solution respectively, $n$ is the refractive index of the solvents, $D$ is the integrated intensity, and $\Phi$ is the luminescence quantum yield. The quantity $B$ is calculated by $B = 1 - 10^{-AL}$, where $A$ is the absorbance at the excitation wavelength and $L$ is the optical path length. Solid-state emission quantum yields ($\Phi_{ss}$) of samples were measured by the method of Wrighton[20] with KBr as the standard and calculated by $\Phi_{ss} = E/(R_{std} - R_{smpl})$, where the subscript ss refers to solid-state, $E$ is the area under the corrected emission curve of the sample and $R_{std}$ and $R_{smpl}$ are the corrected areas under the diffuse reflectance curves of the non-absorbing standard and the sample, respectively, at the excitation wavelength.

Cyclic voltammetry was performed using a PAR model 175 universal programmer and a Model 173 potentiostat. Cyclic voltammograms were recorded with a Kipp & Zonen BD90 X-Y recorder at scan rates of 50 mV s$^{-1}$. The electrolytic cell used was a conventional two compartments cell. Electrochemical measurements were performed at room temperature after purging with nitrogen using 0.1 M tetrabutylammonium hexafluorophosphate (TBAP)/dimethylformamide as supporting electrolyte. The working electrode was a glassy carbon (Atomergic Chemetal V25, geometric area of 0.35 cm$^2$) electrode and the counter electrode was platinum gauze. A nonaqueous $Ag/AgNO_3$ (0.1 M in acetonitrile) reference electrode was contained in a separate compartment connected to the test solution via fine sintered glass disks. The ferrocenium/ferrocene couple was used as the internal standard.

**Electroluminescence:** The single-layer films were prepared by spin-coating a solution of the Pt complex (10 wt%) and PVK (90 wt%) in chloroform (total wt% of solids was 10 mg/ml) onto quartz substrate. The single-layer EL devices were made in air by spin-coating a solution of the Pt complexes (10 wt%) and PVK (90 wt%) in chloroform (total wt% of solids was 10 mg/ml) onto ITO-coated glass (resistivity = 20 Ω cm$^{-2}$). A layer of aluminum (200 nm) was deposited as the cathode. For the double-layer EL devices, after the PVK:**Pt** layer was spin-coated onto ITO-coated glass (resistivity = 20 Ω cm$^{-2}$), PBD was deposited by thermal evaporation at normal deposition rate of 0.5 nm s$^{-1}$. This was followed by deposition of the aluminum cathode. The thickness of the PBD layer and aluminum layers are 400 and 200 nm, respectively. The EL and PL spectra were recorded in air with a Shimadzu RF-5301 PC spectrometer.

**Synthesis: [Pt(5,5′-dmbpy)(C≡CPh)$_2$] (2a)**: The method of Sonogashira was adopted.[12] [Pt(5,5′-dimethyl-2,2′-bipyridine)$Cl_2$] (0.20 g, 0.44 mmol), CuI (0.01 g, 0.05 mmol), and diisopropylamine (1 mL) were added to dichloromethane (20 mL) and the resultant mixture was stirred for 10 min. After the addition of freshly distilled phenylacetylene (0.15 g, 1.78 mmol), the mixture was stirred at room temperature for 18 h. The yellow mixture was evaporated to dryness, dissolved in dichloromethane, and loaded onto an alumina column (15 × 2 cm) with dichloromethane as eluent. The product was eluted as a yellow band (2nd fraction) which was evaporated to dryness. The solid was recrystallized by slow diffusion of diethyl ether into a dichloromethane solution to give yellow crystals. Yield: 0.19 g, 74%. $^1$H NMR ($CD_2Cl_2$): $\delta = 9.48$ (s, 2H; py-H$^6$), 7.93 (m, 4H; py-H$^{3,4}$), 7.48 (d, $J = 7.2$ Hz, 4H; Ph-H$^2$), 7.30 (t, $J = 7.5$ Hz, 4H; Ph-H$^3$), 7.19 (t, $J = 7.4$ Hz, 2H; Ph-H$^4$), 2.46 (s, 6H; Me); $^{13}$C NMR ($CD_2Cl_2$): $\delta = 154.3$, 151.6, 139.8, 138.4, 132.3, 128.8, 128.5, 126.1, 122.6, 102.2 ($C_\alpha$), 88.4 ($C_\beta$), 19.3 (Me); IR (KBr): $\tilde{\nu}_{C\equiv C} = 2120$, 2109 cm$^{-1}$; Raman: $\tilde{\nu}_{C\equiv C} = 2121$, 2110 cm$^{-1}$; MS-FAB$^+$ (*m*-NBA): *m/z*: 582 $[M]^+$; elemental analysis calcd (%) for $C_{28}H_{22}N_2Pt$ (581.6): C 57.83, H 3.81, N 4.82; found: C 57.53, H 3.78, N 4.51.

**[Pt(4,4′-dtbpy)(C≡CPh)$_2$] (2b)**: The synthesis was similar to that of **2a**, except that [Pt(4,4′-di-*tert*-butyl-2,2′-bipyridine)$Cl_2$] (0.20 g, 0.37 mmol) and phenylacetylene (0.15 g, 1.50 mmol) were used. Yield: 0.21 g, 84%. $^1$H NMR ($CD_2Cl_2$): $\delta = 9.54$ (d, $J = 6.0$ Hz, 2H; py-H$^6$), 8.32 (d, $J = 1.7$ Hz, 2H; py-H$^3$), 7.75 (dd, $J = 6.0$ Hz, $J = 2.1$ Hz, 2H; py-H$^5$), 7.41 (m, 4H; Ph-H$^2$), 7.29 (m, 4H; Ph-H$^3$), 7.20 (m, 2H; Ph-H$^4$), 1.45 (s, 18H; *t*Bu); IR (KBr): $\tilde{\nu}_{C\equiv C} = 2124$, 2114 cm$^{-1}$; Raman: $\tilde{\nu}_{C\equiv C} = 2121$, 2108 cm$^{-1}$; MS-FAB$^+$ (*m*-NBA): *m/z*: 665 $[M]^+$; elemental analysis calcd (%) for $C_{34}H_{34}N_2Pt \cdot CH_2Cl_2$ (750.7): C 56.00, H 4.83, N 3.73; found: C 56.18, H 4.86, N 3.31.

**[Pt(4,4′-dmbpy)(C≡CPh)$_2$] (2c)**: The procedure was similar to that for **2a**, except that [Pt(4,4′-dimethyl-2,2′-bipyridine)$Cl_2$] (0.08 g, 0.44 mmol) and phenylacetylene (0.18 g, 1.78 mmol) were used. Yield 0.14, 55%. $^1$H NMR ($CD_2Cl_2$): $\delta = 9.45$ (d, $J = 5.3$ Hz, 2H; py-H$^6$), 7.93 (s, 2H; py-H$^3$), 7.47 (m, 4H; Ph-H$^2$), 7.35 (d, $J = 5.3$ Hz, 2H; py-H$^5$), 7.28 (m, 4H; Ph-H$^3$), 7.18 (m, 2H; Ph-H$^4$), 2.50 (s, 6H; Me); $^{13}$C NMR ($CD_2Cl_2$): $\delta = 156.1 - 123.8$ (py and Ph), 101.5 ($C_\alpha$), 87.6 ($C_\beta$), 21.9 (Me); IR (KBr): $\tilde{\nu}_{C\equiv C} = 2125$, 2115 cm$^{-1}$; Raman: $\tilde{\nu}_{C\equiv C} = 2127$, 2116 cm$^{-1}$; MS-FAB$^+$ (*m*-NBA): *m/z*: 581 $[M]^+$; elemental analysis calcd (%) for $C_{28}H_{22}N_2Pt$ (581.6): C 57.83, H 3.81, N 4.82; found: C 57.47, H 3.65, N 4.56.

**[Pt(4,4′-dpbpy)(C≡CPh)$_2$] (2d)**: The method reported by Cross et al was modified.[13] Complex **1** (0.20 g, 0.40 mmol) and 4,4′-diphenyl-2,2′-bipyridine (0.13 g, 0.42 mmol) were ground together, added to acetonitrile (60 mL), and stirred at reflux for 3 h. The resulting dark brown mixture was evaporated to dryness. The solid was dissolved in dichloromethane and loaded onto an alumina column. The product was eluted in dichloromethane as a yellow band (2nd fraction). The crude product was recrystallized by slow diffusion of diethyl ether into a dichloromethane solution. Yield: 0.14 g, 50%. $^1$H NMR ($CD_2Cl_2$): $\delta = 9.73$ (d, $J = 5.8$ Hz, 2H; py-H$^6$), 8.39 (d, $J = 1.7$ Hz, 2H; py-H$^3$), 7.83 (m, 6H; py-H$^5$; Ph-H$^3$ of bpy), 7.57 (m, 6H; Ph-H$^{2,4}$ of bpy), 7.46 (dd, $J = 8.2$ Hz, $J = 1.2$ Hz, 4H; Ph-H$^2$), 7.28 (dt, $J = 6.5$ Hz, $J = 1.6$ Hz, 4H; Ph-H$^3$), 7.18 (tt, $J = 7.4$ Hz, $J = 1.8$ Hz, $J = 1.2$ Hz, 2H; Ph-H$^4$); IR (KBr): $\tilde{\nu}_{C\equiv C} = 2124$ (s), 2113 (s) cm$^{-1}$; MS-FAB$^+$ (*m*-NBA): *m/z*: 707 $[M + H]^+$; elemental analysis calcd (%) for $C_{38}H_{26}N_2Pt$ (705.7): C 64.67, H 3.71, N 3.97; found: C 64.16, H 3.41, N 3.77.

**[Pt(tmphen)(C≡CPh)$_2$] (3a)**: The synthesis was similar to that of **2d**, except that 3,4,7,8-tetramethyl-1,10-phenanthroline (94 mg, 0.40 mmol) replaced 4,4′-diphenyl-2,2′-bipyridine. Yield: 0.16 g, 64%. $^1$H NMR ($CD_2Cl_2$): $\delta = 9.52$ (s, 2H; phen-H$^{2,9}$), 8.06 (s, 2H; phen-H$^{5,6}$), 7.53 (m, 4H; Ph-H$^2$), 7.32(m, 4H; Ph-H$^3$), 7.21 (m, 2H; Ph-H$^4$), 2.71 (s, 6H; Me$^{4,7}$), 2.60 (s, 6H; Me$^{3,8}$); $^{13}$C NMR ($CD_2Cl_2$): $\delta = 151.6$, 146.2, 145.9, 134.5, 132.0, 129.2, 128.7, 128.2, 125.7, 123.6, 101.6 ($C_\alpha$), 88.1 ($C_\beta$), 18.3 (Me), 15.5 (Me); IR (KBr): $\tilde{\nu}_{C\equiv C} = 2123$, 2113 cm$^{-1}$; Raman: $\tilde{\nu}_{C\equiv C} = 2125$, 2115 cm$^{-1}$; MS-FAB$^+$ (*m*-NBA): *m/z*: 634 $[M]^+$; elemental analysis calcd (%) for $C_{32}H_{26}N_2Pt$ (633.7): C 60.66, H 4.14, N 4.42; found: C 60.24, H 4.12, N 4.16.

**[Pt(5,6-dmphen)(C≡CPh)$_2$] (3b):** The procedure was similar to that for **2d**, except that 5,6-dimethyl-1,10-phenanthroline (84 mg, 0.40 mmol) replaced 4,4′-diphenyl-2,2′-bipyridine. Yield: 66 mg, 27%. $^1$H NMR ($CD_2Cl_2$): $\delta = 9.84$ (d, $J = 4.1$ Hz, 2H; phen-H$^{2,9}$), 8.77 (d, $J = 8.5$ Hz, 2H; phen-H$^{4,7}$), 7.89 (dd, $J = 8.5$ Hz, $J = 5.1$ Hz, 2H; phen-H$^{3,8}$), 7.53 (m, 4H; Ph-H$^2$), 7.32 (m, 4H; Ph-H$^3$), 7.21 (m, 2H; Ph-H$^4$), 2.83 (s, 6H; Me); $^{13}$C NMR ($CD_2Cl_2$): $\delta = 150.1$, 135.2 – 123.8 (py and Ph), 102.1 ($C_\alpha$), 87.4 ($C_\beta$), 15.7 (Me); IR (KBr): $\tilde{\nu}_{C\equiv C} = 2134$, 2109 cm$^{-1}$; MS-FAB$^+$ (*m*-NBA): *m/z*: 606 $[M]^+$; elemental analysis calcd (%) for $C_{30}H_{22}N_2Pt$ (605.6): C 59.50, H 3.66, N 4.63; found: C 59.53, H 3.36, N 4.41.

**[Pt(5-mphen)(C≡CPh)$_2$] (3c)**: The synthesis was similar to that of **2d**, except that 5-methyl-1,10-phenanthroline (77 mg, 0.40 mmol) was used instead of 4,4′-diphenyl-2,2′-bipyridine. Yield: 72 mg, 31%. $^1$H NMR ($CD_2Cl_2$): $\delta = 10.01$ (d, $J = 5.1$ Hz, 1H; phen-H$^{2/9}$), 9.91 (d, $J = 5.1$ Hz, 1H; phen-H$^{2/9}$), 8.77 (d, $J = 8.4$ Hz, 1H; phen-H$^{4/7}$), 8.57 (d, $J = 8.2$ Hz, 1H; phen-H$^{4/7}$), 7.99 (dd, $J = 8.4$ Hz, $J = 5.2$ Hz, 1H; phen-H$^{3/8}$), 7.91 (dd, $J = 8.2$ Hz, $J = 5.2$ Hz, 1H; phen-H$^{3/8}$), 7.84 (s, 1H; phen-H$^6$), 7.50 (m, 4H; Ph-H$^2$), 7.30 (m, 4H; Ph-H$^3$), 7.20 (m, 2H; Ph-H$^4$), 2.89 (s, 3H; Me); $^{13}$C NMR ($CD_2Cl_2$): $\delta = 151.0$, 150.4, 147.1, 137.3, 135.8, 135.3, 132.0, 131.1, 130.5, 128.4, 128.2, 126.3, 126.1, 125.8, 102.1 ($C_\alpha$), 86.3 ($C_\beta$), 19.0 (Me); IR (KBr): $\tilde{\nu}_{C\equiv C} = 2122$, 2112 cm$^{-1}$; MS-FAB$^+$ (*m*-NBA): *m/z*: 591 $[M]^+$; elemental analysis calcd (%) for $C_{29}H_{20}N_2Pt$ (591.6): C 58.88, H 3.41, N 4.74; found: C 58.61, H 3.30, N 4.64.



0947-6539/01/0719-4188 $ 17.50+.50/0 *Chem. Eur. J.* **2001**, *7*, No. 19

**[Pt(phen)(C≡CPh)$_2$] (3d)**: The synthesis was similar to that of **2d**, except that 1,10-phenanthroline monohydrate (0.08 g, 0.40 mmol) replaced 4,4′-diphenyl-2,2′-bipyridine. Yield: 0.18 g, 81 %. $^1$H NMR ($CD_2Cl_2$): $\delta = 10.02$ (d, $J = 4.1$ Hz, 2H; phen-H$^{2,9}$), 8.69 (d, $J = 8.2$ Hz, 2H; phen-H$^{4,7}$), 8.06 (s, 2H; phen-H$^{5,6}$), 7.90 (dd, $J = 8.1$ Hz, $J = 5.1$ Hz, 2H; phen-H$^{3,8}$), 7.53 (m, Ph-H$^2$, 4H), 7.31 (m, Ph-H$^3$, 4H), 7.21 (m, Ph-H$^4$, 2H); IR (KBr): $\tilde{\nu}_{C\equiv C} = 2116$, 2105 cm$^{-1}$; MS-FAB$^+$ (*m*-NBA): *m/z*: 578 $[M]^+$; elemental analysis calcd (%) for $C_{28}H_{18}N_2Pt$ (577.54): C 58.23, H 3.14, N 4.85; found: C 58.08, H 3.02, N 4.47.

**[Pt(5-pphen)(C≡CPh)$_2$] (3e)**: The synthesis of **3e** was similar to that of **2d**, except that 5-phenyl-1,10-phenanthroline (103 mg, 0.40 mmol) was used in the place of 4,4′-diphenyl-2,2′-bipyridine. A yellow crystalline solid is obtained by slow evaporation of an acetonitrile solution of the crude product. Yield: 50 mg, 19 %. $^1$H NMR ($CD_2Cl_2$): $\delta = 10.02$ (dd, $J = 5.1$ Hz, $J = 1.3$ Hz, 1H; phen-H$^{2/9}$), 9.98 (dd, $J = 5.2$ Hz, $J = 1.4$ Hz, 1H; phen-H$^{2/9}$), 8.67 (m, 2H; phen-H$^{4,7}$), 7.99 (s, 1H; phen-H$^6$), 7.93 (m, 2H; phen-H$^{3,8}$), 7.60 (virtual s, 5H; Ph-phen), 7.54 (m, 4H; Ph-H$^2$), 7.31(m, 4H; Ph-H$^3$), 7.20 (m, 2H; Ph-H$^4$); IR (KBr): $\tilde{\nu}_{C\equiv C} = 2122$, 2112 cm$^{-1}$; MS-FAB$^+$ (*m*-NBA): *m/z*: 654 $[M]^+$; elemental analysis calcd (%) for $C_{34}H_{22}N_2Pt$ (653.6): C 62.48, H 3.39, N 4.29; found: C 62.09, H 3.30, N 3.79.

**[Pt(4,7-dpphen)(C≡CPh)$_2$] (3f)**: The synthesis of **3f** was similar to that of **2d**, except 4,7-diphenyl-1,10-phenanthroline (135 mg, 0.40 mmol) replaced 4,4′-diphenyl-2,2′-bipyridine. Yield: 0.12 g, 40 %. An orange powder form (**3f$_p$**) was obtained by addition of diethyl ether to a dichloromethane solution of **3f**. A deep orange crystalline form (**3f$_c$**) can be isolated by slow evaporation of an acetonitrile solution of **3f**. $^1$H NMR ($CD_2Cl_2$): $\delta = 10.05$ (d, $J = 5.2$ Hz, 2H; phen-H$^{2,9}$), 8.07 (s, 2H; phen-H$^{5,6}$), 7.90 (d, $J = 5.5$ Hz, 2H; phen-H$^{3,8}$), 7.63 (virtual s, 10H; Ph-phen) 7.54 (m, 4H; Ph-H$^2$), 7.32(m, 4H; Ph-H$^3$), 7.21 (m, 2H; Ph-H$^4$); $^{13}$C NMR ($CD_2Cl_2$): $\delta = 151.1 - 125.7$ (py and Ph), 102.8 ($C_\alpha$), 87.3 ($C_\beta$); IR (KBr): $\nu_{C\equiv C} = 2124$, 2112 cm$^{-1}$; Raman: $\nu_{C\equiv C} = 2120$, 2110 cm$^{-1}$; MS-FAB$^+$ (*m*-NBA): *m/z*: 730 $[M]^+$; elemental analysis calcd (%) for $C_{40}H_{26}N_2Pt$ (729.7): C 65.84, H 3.59, N 3.84; found: C 65.62, H 3.48, N 3.55.

**[Pt(4,4′-dtbpy)(C≡C−C≡CPh)$_2$] (4):** The synthesis was similar to that of **2b**, except that excess PhC≡C−C≡CH was used. Recrystallization by slow diffusion of diethyl ether into a dichloromethane solution produced a yellow powder with a yield of 0.23 g (86 %). $^1$H NMR ($CD_2Cl_2$): $\delta = 9.07$ (d, $J = 6.0$ Hz, 2H; py-H$^6$), 8.13 (d, $J = 1.6$ Hz, 2H; py-H$^3$), 7.56 (dd, $J = 5.9$ Hz, $J = 1.8$ Hz, 2H; py-H$^5$), 7.51 (m, 4H; Ph-H$^2$), 7.33 (m, 6H; Ph-H$^{3,4}$), 1.51 (s, 18H; *t*Bu); $^{13}$C NMR ($CD_2Cl_2$): $\delta = 164.6$, 156.9, 150.9, 132.8, 128.7, 128.1, 125.1, 124.3, 120.6, 87.7 ($C_\alpha$), 83.2 ($C_\beta$), 78.7 ($C_\gamma$), 70.4 ($C_\delta$), 36.3 (*C*Me$_3$), 30.4 (C*Me*$_3$); IR (KBr): $\tilde{\nu}_{C\equiv C} = 2181$, 2067 cm$^{-1}$; Raman: $\tilde{\nu}_{C\equiv C} = 2187$, 2070 cm$^{-1}$; MS-FAB$^+$ (*m*-NBA): *m/z*: 714 $[M]^+$; elemental analysis calcd (%) for $C_{38}H_{34}N_2Pt$ (713.8): C 63.93, H 4.80, N 3.93; found: C 63.58, H 4.82, N 3.76.

**X-ray crystallography:** Crystals of **2b–d** and **3f** were obtained by slow diffusion of diethyl ether into dichloromethane solution. Yellow crystals of **3e** were obtained by diffusion of diethyl ether into an acetonitrile solution. Crystal data and details of collection and refinement for **2d**·$CH_2Cl_2$ and **3e**·$CH_3CN$ are summarized in Table 1. Diffraction experiments were performed using graphite monochromatic $Mo_{K\alpha}$ radiation ($\lambda = 0.71073$ Å) on a Rigaku AFC7R diffractometer (**2b**·$CH_2Cl_2$ and **2d**·$CH_2Cl_2$), and a MAR diffractometer with a 300 mm image plate detector (**2c**, **3e**·$CH_3CN$, and **3f**·$(CH_2Cl_2)_{0.75}$). In the cases of **2b–d** and **3e**·$CH_3CN$, the structures were solved by Patterson methods, expanded by Fourier methods (PATTY),[31] and refined by full-matrix least-squares against *F* using the software package TeXsan[32] on a Silicon Graphics Indy computer. In the case of **3f**·$(CH_2Cl_2)_{0.75}$, the structure was solved by full-matrix least-squares against $F_2$ using the program SHELXL97[33] on PC. Unless otherwise stated, H-atoms at calculated positions with thermal parameters equal to 1.3 (**2b–d** and **3e**·$CH_3CN$) or 1.2 (**3f**·$(CH_2Cl_2)_{0.75}$) times that of the attached C atoms were not refined.

The crystallographic asymmetric unit of **2b**·$CH_2Cl_2$ consists of one formula unit and all 40 non-hydrogen atoms were refined anisotropically. In the case of **2c**, the crystallographic asymmetric unit consists of one half of the complex unit. All 16 non-hydrogen atoms of the complex molecule were refined anisotropically. For **2d**·$CH_2Cl_2$, the crystallographic asymmetric unit consists of one formula unit. One of the phenyl rings was disordered and the C(34), C(35), C(37) and C(38) atoms with occupation number of 0.6 were placed at alternate positions at C(34′), C(35′), C(37′) and C(38′) respectively, where each had 0.4 occupancy. In the least-squares refinement, 38 non-hydrogen atoms were refined anisotropically, the 10 C atoms of the disordered phenyl ring were refined isotropically, and the hydrogens that were bound to the C atoms of the disordered phenyl ring were not included in the calculation. For **3e**·$CH_3CN$, the crystallographic asymmetric unit consists of one formula unit. All 37 non-hydrogen atoms of the complex molecule were refined anisotropically, and the three atoms of the solvent molecule were refined isotropically.

The crystallographic asymmetric unit of **3f**·$(CH_2Cl_2)_{0.75}$ consists of two complex units, and one and a half solvent molecules. One phenyl ring [C(75)–C(80)] of one of the two complex units has large thermal parameters and was restrained to a normal phenyl ring with C–C bond lengths of 1.39 Å and C–C–C angles of 120°. All non-hydrogen atoms were refined anisotropically.

Crystallographic data (excluding structure factors) for the structures reported in this paper have been deposited with the Cambridge Crystallographic Data Centre as supplementary publication nos. CCDC-161433 (**2b**·$CH_2Cl_2$), CCDC-161434 (**2c**), CCDC-161435 (**2d**·$CH_2Cl_2$), CCDC-161436 (**3e**·$CH_3CN$), and CCDC-161437 (**3f**·$(CH_2Cl_2)_{0.75}$). Copies of the data can be obtained free of charge on application to CCDC, 12 Union Road, Cambridge CB2 1EZ (UK) (fax: (+44) 1223-336-033; e-mail: deposit@ccdc.cam.ac.uk).

## Acknowledgements

This work was supported by the Research Grants Council of the Hong Kong SAR, China [HKU 7298/99P] and The University of Hong Kong.

[1] a) Y. Fujikura, K. Sonogashira, N. Hagihara, *Chem. Lett.* **1975**, 1067–1070; b) K. Sonogashira, S. Takahashi, N. Hagihara, *Macromolecules* **1977**, *10*, 879–880.

[2] a) J. Manna, K. D. John, M. D. Hopkins, *Adv. Organomet. Chem.* **1995**, *38*, 79–154; b) J. Manna, C. J. Kuehl, J. A. Whiteford, P. J. Stang, D. C. Muddiman, S. A. Hofstadler, R. D. Smith, *J. Am. Chem. Soc.* **1997**, *119*, 11611–11619; c) V. W. W. Yam, K. K. W. Lo, K. M. C. Wong, *J. Organomet. Chem.* **1999**, *578*, 3–30; d) K. Onitsuka, M. Fujimoto, N. Ohshiro, S. Takahashi, *Angew. Chem. Int. Ed.* **1999**, *38*, 689–692; e) P. Nguyen, P. Gómez-Elipe, I. Manners, *Chem. Rev.* **1999**, *99*, 1515–1548; f) N. J. Long in *Optoelectronic Properties of Inorganic Compounds* (Eds.: D. M. Roundhill, J. P. Fackler, Jr.), Plenum Press, New York, **1999**, chapter 4; g) U. Belluco, R. Bertani, R. A. Michelin, M. Mozzon, *J. Organomet. Chem.* **2000**, *600*, 37–55.

[3] a) J. Lewis, M. S. Khan, A. K. Kakkar, B. F. G. Johnson, T. B. Marder, H. B. Fyfe, F. Wittmann, R. H. Friend, A. E. Dray, *J. Organomet. Chem.* **1992**, *425*, 165–176; b) G. Frapper, M. Kertesz, *Inorg. Chem.* **1993**, *32*, 732–740; c) K. A. Bunten, A. K. Kakkar, *Macromolecules* **1996**, *29*, 2885–2893; d) M. Younus, A. Köhler, S. Cron, N. Chawdhury, M. R. A. Al -Mandhary, M. S. Khan, J. Lewis, N. J. Long, R. H. Friend, P. R. Raithby, *Angew. Chem.* **1998**, *110*, 3180–3183; *Angew. Chem. Int. Ed.* **1998**, *37*, 3036–3039; e) N. Chawdhury, A. Köhler, R. H. Friend, W. -Y. Wong, J. Lewis, M. Younus, P. R. Raithby, T. C. Corcoran, M. R. A. Al-Mandhary, M. S. Khan, *J. Chem. Phys.* **1999**, *110*, 4963–4970; f) J. S. Wilson, A. Köhler, R. H. Friend, M. K. Al Suti, M. R. A. Al -Mandhary, M. S. Khan, P. R. Raithby, *J. Chem. Phys.* **2000**, *113*, 7627–7634.

[4] Y. G. Ma, W. H. Chan, X. M. Zhou, C. M. Che, *New J. Chem.* **1999**, 263–265.

[5] a) C. Adachi, M. A. Baldo, S. R. Forrest, M. E. Thompson, *Appl. Phys. Lett.* **2000**, *77*, 904–906; b) C. Adachi, M. A. Baldo, S. R. Forrest, S. Lamansky, M. E. Thompson, R. C. Kwong, *Appl. Phys. Lett.* **2001**, *78*, 1622–1624; c) S. Lamansky, M. E. Thompson, WO 00/57676, **2000**.

[6] For example: a) L. Sacksteder, E. Baralt, B. A. DeGraff, C. M. Lukehart, J. N. Demas, *Inorg. Chem.* **1991**, *30*, 2468–2476; b) H. K. Yip, H. M. Lin, Y. Wang, C. M. Che, *J. Chem. Soc. Dalton Trans.* **1993**, 2939–2944; c) V. W. W. Yam, L. P. Chan, T. F. Lai, *Organometallics* **1993**, *12*, 2197–2202; d) V. W. W. Yam, P. K. Y. Yeung, L. P. Chan, W. M. Kwok, D. L. Philips, K. L. Yu, R. W. K. Wong, H. Yan, Q. J. Meng, *Organometallics* **1998**, *17*, 2590–2596; e) J. P. H. Charmant, J. Forniés, J. Gómez, E. Lalinde, R. I. Merino, M. T. Moreno, A. G.

Orpen, *Organometallics* **1999**, *18*, 3353 – 3358; f) I. Ara, J. R. Berenguer, E. Eguizábal, J. Forniés, J. Gómez, E. Lalinde, J. M. Sáez-Rocher, *Organometallics* **2000**, *19*, 4385 – 4397.
[7] C. W. Chan, L. K. Cheng, C. M. Che, *Coord. Chem. Rev.* **1994**, *132*, 87 – 97.
[8] V. M. Miskowski, V. H. Houlding, C. M. Che, Y. Wang, *Inorg. Chem.* **1993**, *32*, 2518 – 2524.
[9] a) Y. Y. Ng, C. M. Che, S. M. Peng, *New J. Chem.* **1996**, *20*, 781 – 789; b) dimesityl analogues: A. Klein, W. Kaim, *Organometallics* **1995**, *14*, 1176 – 1186.
[10] a) S. L. James, M. Younus, P. R. Raithby, J. Lewis, *J. Organomet. Chem.* **1997**, *543*, 233 – 235; b) C. J. Adams, P. R. Raithby, *J. Organomet. Chem.* **1999**, *578*, 178 – 185; c) C. J. Adams, S. L. James, X. Liu, P. R. Raithby, L. J. Yellowlees, *J. Chem. Soc. Dalton Trans.* **2000**, 63 – 67.
[11] a) M. Hissler, W. B. Connick, D. K. Geiger, J. E. McGarrah, D. Lipa, R. J. Lachicotte, R. Eisenberg, *Inorg. Chem.* **2000**, *39*, 447 – 457; b) W. B. Connick, D. Geiger, R. Eisenberg, *Inorg. Chem.* **1999**, *38*, 3264 – 3265.
[12] K. Sonogashira, Y. Fujikura, T. Yatake, N. Toyoshima, S. Takahashi, N. Hagihara, *J. Organomet. Chem.* **1978**, *145*, 101 – 108.
[13] F. J. Cross, M. F. Davidson, *J. Chem. Soc. Dalton Trans.* **1986**, 1987 – 1992.
[14] C. A. Hunter, J. K .M. Sanders, *J. Am. Chem. Soc.* **1990**, *112*, 5525 – 5534.
[15] a) S. W. Lai, M. C. W. Chan, T. C. Cheung, S. M. Peng, C. M. Che, *Inorg. Chem.* **1999**, *38,* 4046 – 4055; b) S. W. Lai, T. C. Cheung, M. C. W. Chan, K. K. Cheung, S. M. Peng, C. M. Che, *Inorg. Chem.* **2000**, *39,* 255 – 262; c) S. W. Lai, M. C. W. Chan, K. K. Cheung, C. M. Che, *Organometallics* **1999**, *18*, 3327 – 3336; d) M. C. Tse, K. K. Cheung, M. C. W. Chan, C. M. Che, *Chem. Commun.* **1998**, 2295 – 2296; e) W. Lu, M. C. W. Chan, K. K. Cheung, C. M. Che, *Organometallics* **2001**, *20*, 2477 – 2486.
[16] H. Y. Chao, Y. Q. Li, C. M. Che, unpublished results.
[17] H. Masai, K. Sonogashira, H. Hagihara, *Bull. Chem. Soc. Jpn.* **1971**, *44*, 2226 – 2230.
[18] K. T. Wan, C. M. Che, unpublished results.
[19] V. W. W. Yam, S. H. F. Chong, C. C. Ko, K. K. Cheung, *Organometallics* **2000**, *19*, 5092 – 5097.
[20] M. S. Wrighton, D. S. Ginley, D. L. Morse, *J. Phys. Chem.* **1974**, *78*, 2229 – 2233.
[21] V. W. W. Yam, W. K. M. Fung, K. K. Cheung, *Organometallics* **1997**, *16*, 2032-2037.
[22] a) D. J. Stufkens, A. Vlćek Jr., *Coord. Chem. Rev.* **1998**, *177*, 127 – 179; b) M. J. Bakker, F. Hartl, D. J. Stufkens, O. S. Jina, X. -Z. Sun, M. W. George, *Organometallics* **2000**, *19*, 4310 – 4319.
[23] D. Collison, F. E. Mabbs, E. J. L. McInnes, K. J. Taylor, A. J. Welch, L. J. Yellowlees, *J. Chem. Soc. Dalton Trans.* **1996**, 329 – 334.
[24] C. W. Tang, S. A. Van Slyke, C. H. Chen, *J. Appl. Phys.* **1989**, *65*, 3610 – 3616.
[25] W. Lu, B. X. Mi, M. C. W. Chan, Z. Hui, N. Zhu, S. T. Lee, C. M. Che, unpublished results.
[26] D. D. Perrin, W. L. F. Armarego, D. R. Perrin, *Purification of Laboratory Chemicals 2nd ed.*, Pergamon, Oxford, **1983**.
[27] K. D. Hodges, J. V. Rund, *Inorg. Chem.* **1975**, *14*, 525 – 528.
[28] G. M. Badger, W. H. F. Sasse, *J. Chem. Soc.* **1956**, 616 – 620.
[29] A. S. Kende, C. A. Smith, *J. Org. Chem.* **1988**, *53*, 2655 – 2657.
[30] J. N. Demas, G. A. Crosby, *J. Phys. Chem.* **1971**, *75*, 991 – 1024.
[31] PATTY: P. T. Beursken, G. Admiraal, G. Beurskens, W. P. Bosman, S. Garcia -Granda, R. O. Gould, J. M. M. Smits, C. Smykalla, **1992**, The *DIRDIF* program system, Technical Report of the Crystallography Laboratory, University of Nijmegen, The Netherlands.
[32] TeXsan: Crystal Structure Analysis Package, Molecular Structure Corporation, (**1985** & **1992**), The Woodlands, Texas (USA).
[33] SHELXS97: G. M. Shekdrick, SHELX97, **1997**. Programs for Crystal Structure Analysis (Release 97 – 2). University of Goetingen (Germany).

Received: April 6, 2001 [F3185]

  0947-6539/01/0719-4190 $ 17.50+.50/0 